

Effective Adapter for Face Recognition in the Wild

Yunhao Liu¹, Lu Qi^{2*}, Yu-Ju Tsai², Xiangtai Li³, Kelvin C.K. Chan⁴, Ming-Hsuan Yang^{2,4},

¹Dalian University of Technology ²The University of California, Merced

³Nanyang Technology University ⁴Google Research

<https://liuyunhaozz.github.io/faceadapter/>

Abstract

In this paper, we tackle the challenge of face recognition in the wild, where images often suffer from low quality and real-world distortions. Traditional heuristic approaches—either training models directly on these degraded images or their enhanced counterparts using face restoration techniques—have proven ineffective, primarily due to the degradation of facial features and the discrepancy in image domains. To overcome these issues, we propose an effective adapter for augmenting existing face recognition models trained on high-quality facial datasets. The key of our adapter is to process both the unrefined and the enhanced images by two similar structures where one is fixed and the other trainable. Such design can confer two benefits. First, the dual-input system minimizes the domain gap while providing varied perspectives for the face recognition model, where the enhanced image can be regarded as a complex non-linear transformation of the original one by the restoration model. Second, both two similar structures can be initialized by the pre-trained models without dropping the past knowledge. The extensive experiments in zero-shot settings show the effectiveness of our method by surpassing baselines of about 3%, 4%, and 7% in three datasets. Our code will be publicly available at <https://github.com/liuyunhaozz/FaceAdapter/>.

1. Introduction

In recent years, deep learning [26, 27, 32, 44, 58–64, 71, 73, 74, 93, 94] techniques have achieved remarkable progress in the field of face recognition [13, 17, 43, 51, 53, 81, 83, 91]. This advancement has profoundly benefited various applications like financial services [34, 41, 69], greatly enhancing security and convenience in identity verification processes [75, 76].

Despite these advancements, face recognition in real-

world scenarios [31, 54, 56], often termed as *recognition in the wild*, still poses significant challenges. The primary issue lies in the discrepancy between the high-quality images used in the training period and the lower-quality images typically encountered in everyday settings. These real-world images often suffer from various distortions and degradation, such as blurring or poor resolution, creating a substantial image domain gap [18, 37]. This gap significantly affects the effectiveness and reliability of face recognition systems, thereby hindering their broader deployment in practical applications.

An intuitive way to address this challenge is employing face restoration [25, 45, 48, 88, 92] models to enhance low-quality images into high-quality ones. However, we observe that this denoising process can further increase the domain gap in real-world scenarios. Another potential solution involves training a face recognition model from scratch or fine-tuning [78, 97] it on these enhanced images. However, they would lose vital information from the original images, as restoration models do not consistently achieve perfect recovery. Therefore, retaining the original low-quality images in conjunction with the enhanced ones is essential, ensuring that the model remains the original image domain encountered in real-world settings.

Based on the analysis above, we introduce an adapter framework designed to enhance face recognition in real-world (wild) conditions. The key to this framework is an adapter design integrated with a pre-trained face recognition model. Such a design harnesses the capabilities of existing face restoration models by applying the adapter to enhance high-quality images. Specifically, our framework employs a dual-branch structure: the adapter processes the restored images, and the frozen, pre-trained face recognition model handles the original low-quality images. After that, we propose a novel fusion module to ensemble the features of both two views by nested Cross- and Self-Attention mechanisms. Last, the fused features are used for similarity calculation.

We conduct comprehensive experiments in a simulated real-world environment commonly used in image restora-

*Corresponding author

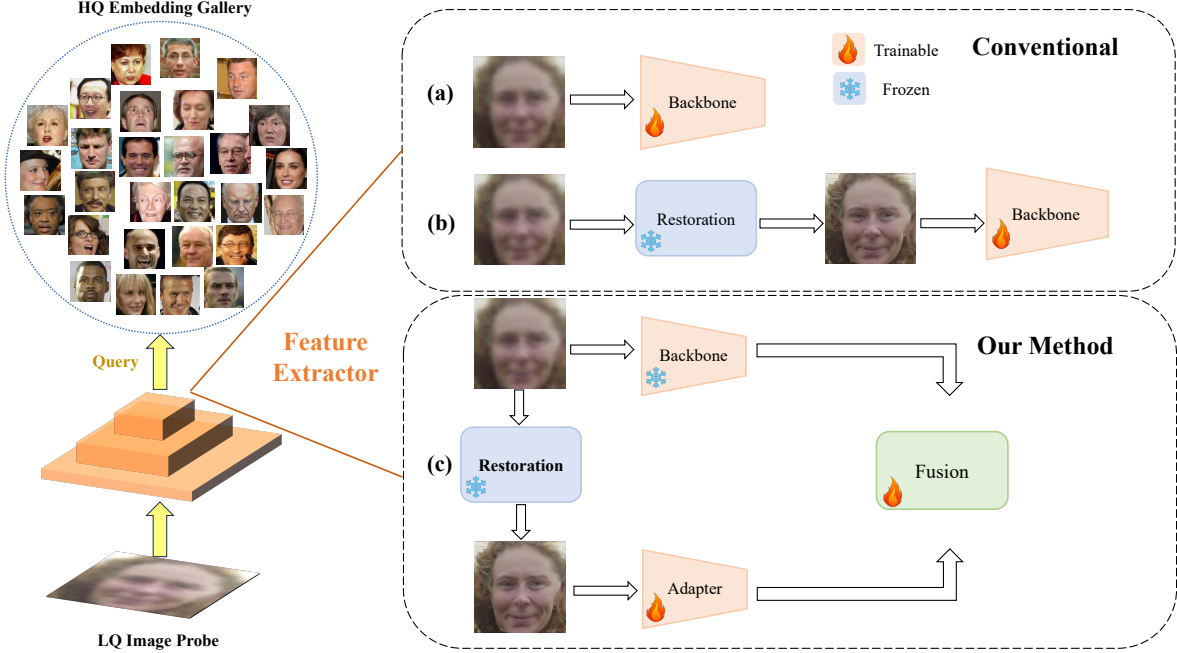


Figure 1. In real-world applications, face recognition systems frequently encounter probe images of low quality (LQ), which presents a significant domain gap compared to the high-quality (HQ) embedding gallery. Our method (c) addresses this challenge by integrating the features from the LQ images with those of enhanced HQ images in the fusion structure. Compared with conventional methods (a) (b), our method effectively bridges the domain gap, ensuring more accurate and reliable face recognition performance in real-world conditions.

tion and domain adaptation studies. We train our model on one face recognition dataset and then test its effectiveness on the other three additional ones in a zero-shot manner. This approach enables us to demonstrate the robustness and adaptability of our adapter framework in the wild. Fig. 1 provides an overview of our approach.

Our main contribution is concluded as follows:

- We propose a novel framework for face recognition in the wild. It simultaneously processes low-quality and high-quality images enhanced by the face restoration model, bridging the gap between different image domains.
- The key to our face recognition framework is an adaptor design that the pre-trained model on high-quality images can initialize. It allows the model to adapt low-quality images without training from scratch quickly. In this way, the adaptor design keeps the original performance of low-quality images as the lower bound.
- With the help of Cross-Attention and Self-Attention mechanisms, the extensive experiments show the considerable accuracy and reliability of the recognition process in the wild.

2. Related Work

2.1. Face Recognition Methods

Recent advancements in deep learning (DL) have significantly propelled the field of face recognition (FR). Historically, before the advent of deep learning, face recognition is reliant on manually designed features with methods such as Eigenface [5] and Fisherface [2]. The integration of deep learning has revolutionized this field, with a focus on model training and testing involving various network architectures. Recent algorithms in face recognition are categorized based on several factors including the design of the loss function [16, 17, 19, 36, 50, 52, 53, 65, 77, 80, 81, 95], as well as the representation and refinement of embedding [13, 30, 35, 38, 43, 55, 79, 83, 91]. Building on the advancements in deep learning for face recognition, our research specifically targets face recognition under low-quality image conditions.

2.2. Face Restoration Methods

Face Restoration (FR) aims to convert low-quality (LQ) facial images into high-quality (HQ) counterparts. Traditional methods relied on statistical priors and degradation models [3, 8, 23, 49, 70, 82, 90] but often fell short in practical applications. The advent of deep learning has led to signifi-

cant progress in this field. Recent research in deep learning-based [9, 10, 25, 39, 45, 48, 85, 89, 92, 96, 98] face restoration methods includes a variety of techniques, network architectures, loss functions, and benchmark datasets. These advances are crucial in addressing challenges in face recognition. However, the Face recognition model trained with restored images suffers from domain gap problems in recognizing low-quality images. To address this, our model adopts a dual-input approach, integrating information from both low- and high-quality images.

2.3. Face Recognition in Low-Quality Images

Face recognition in low-quality images has become increasingly important, especially in video surveillance and other real-world scenarios where capturing high-quality images may not be feasible. Research in this area has been categorized into four main approaches [47]: (i) super-resolution based methods [20, 40, 86], (ii) methods employing low-resolution robust features [6, 22, 29, 84], (iii) methods learning a unified representation space [1, 7, 46, 66, 87], and (iv) remedies for blurriness [15, 21, 42, 72]. Most of these methods are non-deep learning based and typically focus either on low- or high-quality image data, but not both. In this paper, we propose an adapter for augmenting existing face recognition models.

3. Approach

As shown in Fig. 2, we propose a joint face recognition framework that takes dual inputs with two parallel branches. The *LQ Branch*, designed to process original low-quality images, remains frozen to provide a stable feature extraction baseline. In contrast, the *HQ Branch*, dedicated to handling restored high-quality (HQ) images enhanced by the restoration model, is dynamically trained to adapt and extract distinct features. We further design a novel fusion structure with nested Cross-Attention and Self-Attention mechanisms to combine features from both branches. Then, we train our fusion structure through Angular Margin Softmax for accurate loss calculation. By merging the LQ feature from the pre-trained recognition model and the HQ feature from our adapter, our approach presents a comprehensive and robust solution for reliable face recognition in real-world environments.

3.1. Joint Face Recognition

LQ Branch. This branch aims to extract features from low-quality images using a pre-trained recognition model trained on large-scale datasets. Benefiting from the priors induced by large-scale datasets, the model offers robust feature representations and serves as our design’s foundational model, enabling us to adapt to new image degradation efficiently. As such, this model is crucial in our framework because it ensures that the subsequent training of other model

components does not degrade the overall recognition performance. In our work, we choose Arcface [17] as our pre-trained face recognition model that uses the ResNet-50 [28] as its backbone network. Given a low-quality image, we use the pre-trained recognition model to extract the corresponding feature, denoted as $\mathcal{F}_f \in \mathbb{R}^{B \times 512}$ where B is the image numbers in a batch.

HQ Branch. While we have a baseline with a pre-trained face recognition model, we notice a significant drop in accuracy when using low-quality images as input. This degraded accuracy contrasts with the high accuracy achieved by using high-quality images as input. This observation motivates us to design an HQ branch with high-quality inputs, which the face restoration model restores.

We need to use the face restoration method first to obtain high-quality images from low-quality images. However the domain gap still exists between real HQ images and restored images, so we can not directly use the pre-trained face recognition model for verification. To address this domain gap, we design a trainable HQ branch with an identical structure to the LQ branch.

The HQ Branch is an essential component of our framework, primarily focused on extracting features from high-quality images restored from their original, lower-quality versions. Similar to the LQ Branch, the HQ Branch also employs ResNet-50 architecture. The usage of the same backbone for both models offers several advantages. Firstly, it ensures consistency in the type of features extracted from both high and low-quality images, facilitating a more streamlined fusion process. Secondly, employing the same architecture in both branches offers the significant advantage of weight initialization. By initializing the HQ Branch with weights from Arcface, we provide a robust starting point for the model’s training. This initialization is particularly beneficial because it leverages a well-established network’s pre-learned patterns and features and leads to quicker convergence and improved performance.

A key distinction of the HQ Branch is that its parameters are open for training. This trainable part allows the adapter model to dynamically learn and refine the features specific to the restored high-quality images, thereby improving the model’s ability to access the domain of restored images. The feature vector obtained post-training in the trainable adapter aligns with that of the frozen backbone, represented as $\mathcal{F}_a \in \mathbb{R}^{B \times 512}$, where \mathcal{F}_a denotes the feature vector from the Face adapter Model.

3.2. Fusion Structure

This section focuses on the methodology for fusing features from the LQ Branch with those from the HQ Branch. Our approach employs a multi-layered structure of Cross-Attention and Self-Attention mechanisms. This nested fusion technique allows for a more nuanced and context-

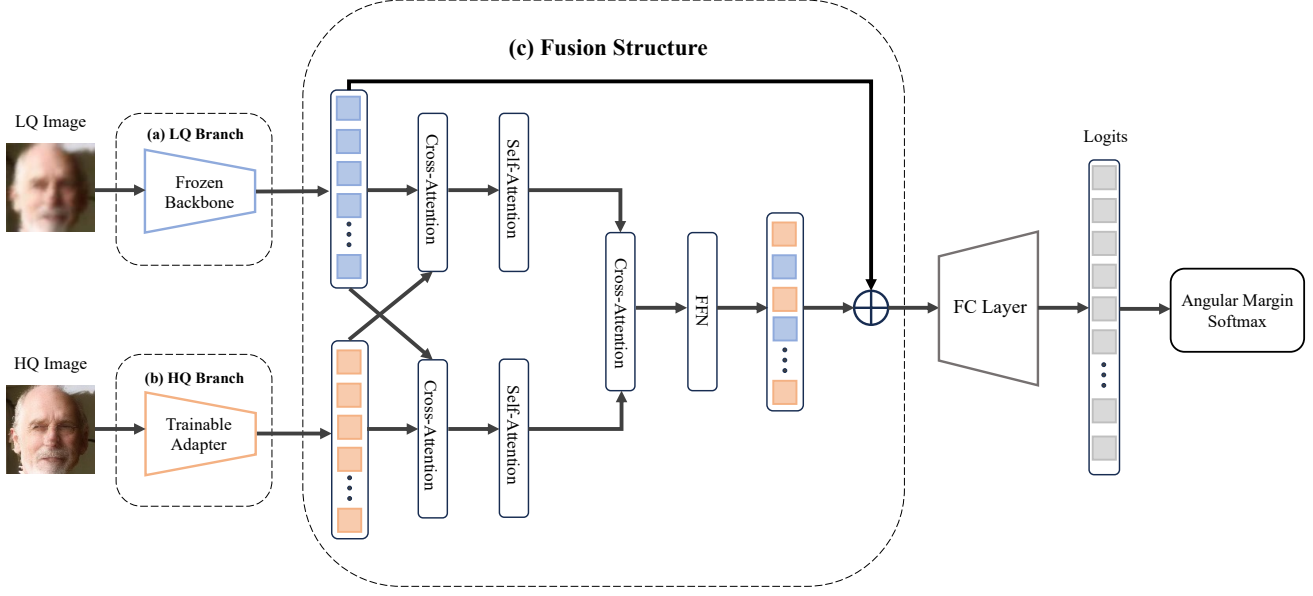


Figure 2. **Joint Face Recognition Framework with Dual-Input Processing.** This architecture processes both low-quality (LQ) and restored high-quality (HQ) images, extracting them by two identical face recognition models. The Fusion Structure integrates feature sets before passing them to an Angular Margin Softmax function for loss computation, optimizing the network for enhanced recognition accuracy.

aware integration of features.

Dual Cross-Attention. In this initial stage of the Fusion Structure, we focus on integrating features generated by the frozen backbone (\mathcal{F}_f) and the trainable adapter (\mathcal{F}_a). We swap the positions of these two sets of features in the two identical Cross-Attention layers respectively, followed by two identical Self-Attention Layers. This produces two sets of values, which are formulated as follows:

1) The first feature set, \mathcal{F}_{aff} , is defined by:

$$\mathcal{F}_{\text{aff}} = \text{SA}_1(\text{CA}_1(\underbrace{g_q(\mathcal{F}_a)}_{\text{query}}, \underbrace{g_k(\mathcal{F}_f)}_{\text{key}}, \underbrace{g_v(\mathcal{F}_f)}_{\text{value}})) \quad (1)$$

2) The second feature set, \mathcal{F}_{faa} , is given by:

$$\mathcal{F}_{\text{faa}} = \text{SA}_2(\text{CA}_2(\underbrace{g_q(\mathcal{F}_f)}_{\text{query}}, \underbrace{g_k(\mathcal{F}_a)}_{\text{key}}, \underbrace{g_v(\mathcal{F}_a)}_{\text{value}})) \quad (2)$$

Here, the statements $\text{SA}_{1,2}(\cdot)$ and $\text{CA}_{1,2}(\cdot)$ represent distinct instances of the same underlying Self-Attention and Cross-Attention model. $g_{\{q,k,v\}}(\cdot)$ are the linear transformations to generating the query, key, and value in the attention process. This stage is crucial for merging the distinct information from both low and high-quality images, enhancing the model's ability to recognize faces with greater accuracy and robustness.

Single Cross-Attention. We have already obtained two feature sets, \mathcal{F}_{aff} and \mathcal{F}_{faa} . The set \mathcal{F}_{aff} is derived where high-quality features are used as the query, and \mathcal{F}_{faa} is where

low-quality features serve as the query, both resulting from the Dual Cross-Attention mechanism. In this stage, we apply another single layer of Cross-Attention followed by a Feed Forward Network (FFN), further refining and fusing the features. This is mathematically represented as:

$$\mathcal{F}_{\text{fusion}} = \text{FFN}(\text{CA}_3(\underbrace{g_q(\mathcal{F}_{\text{aff}})}_{\text{query}}, \underbrace{g_k(\mathcal{F}_{\text{faa}})}_{\text{key}}, \underbrace{g_v(\mathcal{F}_{\text{faa}})}_{\text{value}})) \quad (3)$$

Here, CA_3 is an instance of the Cross-Attention model. The utilization of \mathcal{F}_{aff} as the query in this second stage is a strategic choice. It ensures that the fusion process continues to prioritize and effectively utilize the detailed information from the high-quality recovered images, which is essential for enhancing the accuracy and reliability of the final fused feature set for face recognition.

Residual Structure. The integral Residual Structure in our model is designed to enhance the robustness of the face recognition system by incorporating stable features from the Face Freeze Model with the dynamic features from the Fusion Structure. The mathematical formulation of the Residual Structure is as follows:

$$\mathcal{R} = \mathcal{F}_f + \mathcal{F}_{\text{fusion}} \quad (4)$$

Where \mathcal{R} represents the resultant residual feature, \mathcal{F}_f is the feature vector from the LQ Branch, and $\mathcal{F}_{\text{fusion}}$ symbolizes the fused feature vector generated by the nested attention mechanisms mentioned before. The LQ Branch,

Methods	LFW (20k)	CFP-FP (20k)	AgeDB (20k)
Arcface (0.5)	98.500	90.157	92.350
Cosface (0.35)	99.033	93.371	93.117
QAface (0.5)	98.317	90.629	80.667
Ours (Arcface)	99.133	91.529	93.850
Ours (Cosface)	99.400	93.886	94.317
Ours (QAface)	99.167	93.314	87.350

Table 1. Verification results (%) of different face recognition models on LFW, CFP-FP, and AgeDB datasets under 20k blurring intensity. For methods Arcface, Cosface, and QAface, we directly test LQ images on their pre-trained model. For our method, we use both LQ and HQ images as input.

characterized by its frozen, pre-trained backbone, provides a stable and consistent feature set. Adding these features to the fusion output ensures that the final feature representation retains a baseline level of quality and reliability.

The Residual Structure’s utility lies in anchoring the feature set, mitigating potential variabilities introduced during the fusion process. This ensures that the final feature representation does not diverge significantly from a dependable baseline, a crucial aspect in scenarios involving highly variable or uncertain fusion outcomes.

3.3. Training Objective

Angular Margin Softmax. In this section, we elaborate on the Angular Margin Softmax [17] loss function, which is integral to our model’s ability to distinguish between different faces effectively. Our implementation utilizes specific parameters: $m_1 = 1.0$, $m_2 = 0.5$, $m_3 = 0.0$, and $s = 64$. These parameters are essential in defining the loss function, formulated as follows:

$$L = -\frac{1}{N} \sum_{i=1}^N \log \frac{e^{s \cdot \cos(m_1 \cdot \theta_{y_i} + m_2) - m_3}}{e^{s \cdot \cos(m_1 \cdot \theta_{y_i} + m_2) - m_3} + \sum_{j=1, j \neq y_i}^n e^{s \cdot \cos \theta_j}} \quad (5)$$

In this formula, θ_{y_i} is the angle between the feature vector and the class center for the correct class y_i , and N represents the number of classes. The parameters m_1 , m_2 , and m_3 modulate the angular distance, with s as the scaling factor. Adopting these parameters in the Angular Margin Softmax loss function enhances our model’s discriminative power, ensuring more distinct and separable feature representations for reliable face recognition in various real-world scenarios.

4. Experiments

4.1. Implementation Details

Datasets. Our experiments utilize the UMDFaces [4] dataset, with 367, 888 images across 8, 277 labels for training, and test on three public datasets: LFW [33] (12, 000 images), CFP-FP [68] (14, 000 images), and AgeDB [57] (12, 000 images).

To simulate the real-world environment in which our model runs, we incorporated a simulation tool, TurbulenceSim [14], to induce image degradation. Our image degradation model includes four distinct parameters: $meters = 10k, 20k, 30k$, and $40k$, representing the turbulence intensity in the algorithm. Larger values indicate greater image blurring. Using this tool, we can apply varied blurring effects to the face images in our dataset, allowing for a controlled experimentation environment. In our face restoration model, we use Codeformer [96] with the fidelity weights $w = 0.5$.

Evaluation Metrics. In our study, we perform zero-shot face verification using our model across three datasets: LFW, CFP-FP, and AgeDB. We adopt a 1 : 1 face recognition verification methodology, wherein the verification set images are divided equally into gallery and probe sets. For gallery images, the pre-trained Arcface backbone is utilized. In contrast, for the probe images, we use our joint framework. Each image and its horizontally flipped version are fed into the model to generate two distinct embeddings, which are then aggregated to form an enriched face representation.

The similarity between probe and gallery image embeddings is assessed using Euclidean distance. A specific threshold, determined by searching values from 0 to 4 in increments of 0.01, is applied to classify whether two faces are identical. The images are deemed a match if the distance falls below this threshold. Each model’s effectiveness is gauged by its accuracy in correctly verifying identities across all image pairs, thus providing a quantifiable measure of its proficiency in face recognition tasks.

4.2. Experimental Settings

Our Joint Framework comprises two parallel branches: the LQ Branch and the HQ Branch. Both branches take the Arcface [17] backbone as the pre-trained weight. We output face features with a dimensionality of 512.

The recognition component of our model utilizes Arcface, with training initiated using a pre-trained Arcface backbone to improve convergence. For face restoration, the CoderFormer model is employed, tasked with generating high-quality images for the HQ Branch.

The training is conducted with a batch size of 256 across 5 epochs, processing images at a resolution of 112×112 . We optimize the model using SGD with an initial learning rate of 0.02, momentum set to 0.9, and weight decay of $5e^{-4}$. The learning rate follows a Polynomial Warmup schedule, which starts with a warmup phase where the learning rate ramps up, followed by a polynomial decay that adjusts the learning rate based on the progress of training epochs. The LQ Branch remains frozen throughout this process, while the HQ Branch and the Fusion Structure, including Self-Attention, Cross-Attention, and the Feed For-

Backbones	LFW (20k)	CFP-FP (20k)	AgeDB (20k)
Arcface	99.133	91.529	93.850
Cosface	99.400	93.886	94.317
QAface	99.167	93.314	87.350

Table 2. Verification results (%) of the model using different face recognition pre-trained backbone on LFW, CFP-FP, and AgeDB Datasets with 20k blurring intensity.

ward Network, are actively trained.

In our comparison experiment, detailed in Table 1, we demonstrate the effectiveness of our model in enhancing the performance of standard face recognition models like Arcface, Cosface, and QAface, especially under conditions of 20k blurring intensity on the LFW, CFP-FP, and AgeDB datasets. The results show that when our approach is applied to these models, there is an improvement in their ability to recognize faces in low-quality images. This enhancement is attributed to our model’s capability to effectively process and combine features from low and high-quality images, thereby enriching the existing face recognition models with an increased capacity to handle image quality degradation. This experiment highlights our approach’s potential as a versatile tool for improving face recognition accuracy in real-world scenarios with low image quality.

4.3. Ablation Study

In this section, we synthesize our findings from a comprehensive evaluation of face recognition systems, addressing the effect of image blurriness, the performance of backbone models under quality variations, the efficacy of feature fusion methods, and the strategic implementation of attention mechanisms. This collective analysis is crucial for understanding and enhancing the system’s resilience and accuracy in diverse conditions.

4.3.1 Joint Face Recognition Framework

Face Restoration In the ablation study of the face restoration model, we choose Codeformer and Restoreformer [89]. Specifically, within the Codeformer framework, we configured three variants with varying image recovery effects by adjusting the fidelity weights $w = 0.0, 0.5, 1.0$. These variations are utilized in the subsequent Ablation Study to evaluate their performance differences.

In Fig. 3, We evaluate four distinct face recovery models on datasets with 10k, 20k, 30k, and 40k blurring intensity, showing that using Restoreformer as the restoration model in our method has the best face recognition accuracy. Notably, CodeFormer’s recognition accuracy improves as the parameter w increases. Consistent with expectations, there is a discernible decrease in face recognition accuracy correlating with increased image blurriness.

Methods	LFW (20k)	CFP-FP (20k)	AgeDB (20k)
w/o Restoration	98.500	90.157	92.350
After Restoration	91.517	79.029	80.750
Fine-tuning	98.717	89.014	86.700
Ours	99.133	91.529	93.850

Table 3. Verification results (%) using four different face recognition strategies on LFW, CFP-FP, and AgeDB Datasets with 20k blurring intensity. We use the same Arcface pre-trained backbone.

Pre-trained Face Recognition Backbone The backbone model in a face recognition system serves as the foundational architecture upon which the performance of the entire system is heavily reliant. In our experiment, we choose to evaluate three prominent backbone models: Arcface [17], Cosface [81], and QAface [67]. These models are selected based on their distinct approaches to handling face recognition tasks and their reported efficacy in existing literature.

As shown in Table 2, our model with the Cosface backbone has achieved the highest accuracy among all tested methods in the specific datasets, with its performance being especially prominent in the AgeDB dataset. This indicates that this particular version of the algorithm is highly effective in face recognition tasks.

Face Recognition strategy. Our ablation study which is shown in Table 3 compares four strategies for face recognition in the real world. For these four experiments, we all use Arcface as the pre-trained face recognition backbone.

- **Evaluation without Restoration:** Compute the face features directly on the pre-trained model without restoration.
- **Evaluation after Restoration:** Compute the restored face features directly on the pre-trained model after restoration.
- **Fintune with restored images:** Use the restored images to fine-tune the pre-trained model and compute restored face features.
- **Our Method:** Adapting Joint Face Recognition Framework to fuse low-quality face features and recovered features simultaneously.

The Evaluation Method shows that performance drops very fast when directly applied to restored images because there is a significant domain gap between the original and restored images. Fine-tuning the model on restored images does show improvement, as the model adjusts to the data’s diminished quality. However, the problem of domain gap still exists, because the model lacks the information of origin low-quality images after training. Our fusion structure approach, which combines features from both low-quality and restored images through a dual input network, significantly outperforms the other methods.

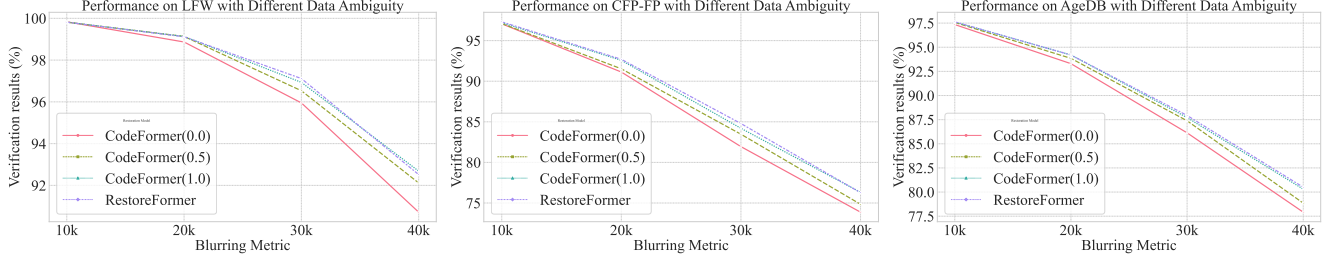
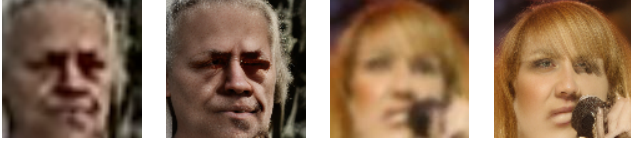
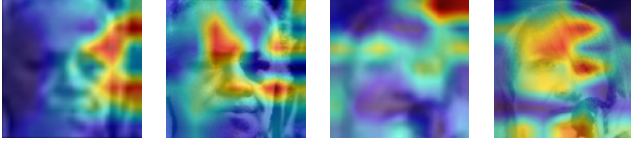


Figure 3. Verification performance (%) using different face restoration methods on LFW, CFP-FP, and AgeDB with different Blurring Intensity.



(a) Two sets of low-quality images and the restored high-quality images using CoderFormer (w=0.5).



(b) Heat map corresponding to the image in (a), aligned by columns.

Figure 4. We use GramCAM [24] for feature visualization of low-quality images and recovered images fed into the face recognition model.

Methods	LFW (20k)	CFP-FP (20k)	AgeDB (20k)
w/o Residual	98.567	91.614	93.383
With Residual (Ours)	99.133	91.529	93.850

Table 4. Verification results (%) of models with and without residual structure in LFW, CFP-FP, and AgeDB datasets at 20k blurring intensity.

4.3.2 Fusion Structure

Residual Structure. As shown in Table 4, The second part of our ablation study within the feature fusion strategy examines the effect of implementing a residual structure during the fusion phase. The residual structure is designed to integrate the embedding from the LQ Branch trained on restored high-quality images into the fusion features obtained from our Fusion Structure.

The experimental results show higher face recognition accuracy with residual structure under LFW and AgeDB datasets and the increase is more pronounced. This indicates that the residual structure plays a role in our model. The residual structure utilizes the features generated by the pre-trained, frozen backbone. This integration ensures the baseline quality of the feature.

Methods	LFW (20k)	CFP-FP (20k)	AgeDB (20k)
Cascade $\times 5$	50.800	50.071	50.000
Cascade $\times 3$	99.100	91.329	93.317
No Cascade (Ours)	99.133	91.529	93.850

Table 5. Verification performance (%) using different cascade layers of fusion structure on LFW, CFP-FP, and AgeDB with 20k blurring intensity.

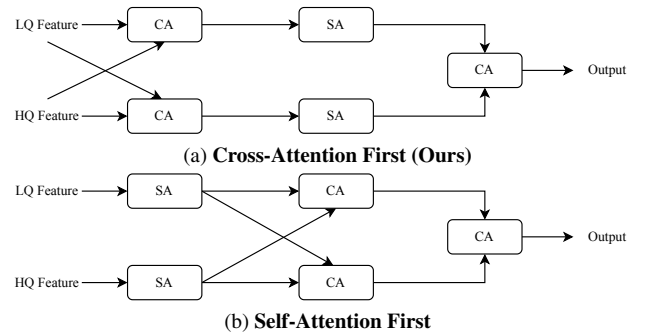


Figure 5. Comparison between the two different attention orders in Fusion Structure. Our method uses (a) Cross-Attention First.

Cascade Structure. Table 5 shows the effect of introducing a cascade structure, which involves repeating our feature fusion method in successive stages. We hypothesize that a multi-layered fusion might enhance recognition accuracy by iteratively refining features.

Contrary to expectations, our experiments show that cascading the fusion process three times did not improve results but maintained or slightly reduced performance compared to our primary fusion method. This suggests that increasing the complexity with additional fusion stages does not necessarily benefit the face recognition system and that a single-stage fusion is sufficient for optimal performance. These outcomes highlight the delicate balance between model complexity and efficacy, advocating for simplicity when additional layers do not contribute to performance gains.

Orders of Attention Mechanisms. Fig. 5 shows two different orders of Self-Attention and Cross-Attention within

Methods	LFW (20k)	CFP-FP (20k)	AgeDB (20k)
Cross-Attention First (Ours)	99.133	91.529	93.850
Self-Attention First	99.100	91.500	93.583

Table 6. Comparison of face recognition accuracy (%) between Cross-Attention First (**Ours**) method and Self-Attention First method across LFW, CFP-FP, and AgeDB datasets at 20k blurring intensity.

our fusion structure, which processes parallel lines of low-quality and high-quality features.

- **Cross-Attention First:** Two successive Cross-Attention layers—one where the low-quality feature line serves as the Query and the high-quality line as Key and Value, followed by the reverse—precede two Self-Attention layers within each line. The sequence concludes with a final Cross-Attention layer to synthesize the fusion feature.
- **Self-Attention First:** Begins with Self-Attention applied within each line independently. This is succeeded by two Cross-Attention layers similar to the First Order, with an additional Cross-Attention layer following them to integrate the final fusion feature.

Table 6 presents a comparative analysis of face recognition accuracy between two attention sequence methodologies across the LFW, CFP-FP, and AgeDB datasets under a 20k blurring intensity. The results indicate that both methods achieve remarkably similar performance across all three datasets. The close proximity in the results of the two methodologies suggests that the nested attention mechanism in our model is efficiently capturing and utilizing the necessary information for face recognition, regardless of the order of the Cross-Attention and Self-Attention layers.

This observation implies that the ability of our model to process and integrate features effectively is not significantly influenced by the alteration in the sequence of attention mechanisms. Consequently, this finding underscores the robustness and flexibility of our nested attention approach, demonstrating its capability to maintain high performance even when the order of attention layers is varied.

Orders of Input in Cross-Attention. In this segment of our study on Cross-Attention mechanisms, we conduct an ablation study to discern the optimal configuration of the Query, Key, and Value roles within a Cross-Attention layer that processes high and low-quality image features.

In the Cross-Attention method of Fusion Structure, the input Feature as Query or Key and Value affects the result. Therefore we test both methods of single Cross-Attention and both methods of nested Cross-Attention. The structure is shown in Fig. 6. We design four experimental setups.

- (a) Use low-quality features as Query and high-quality features as Key and Value.
- (b) Use high-quality features as Query and low-quality features as Key and Value.

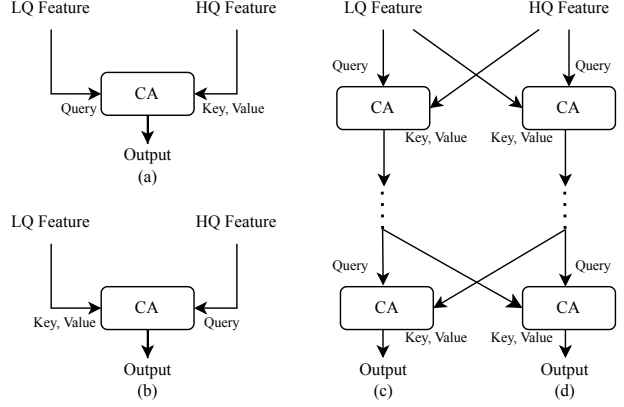


Figure 6. Comparison of methods for different orders of input in Cross-Attention: (a), (b) are the methods for Feature as Query or Key and Value in single Cross-Attention input. (c), (d) are methods in nested Cross-Attention.

Methods	LFW (20k)	CFP-FP (20k)	AgeDB (20k)
(a)	98.883	90.286	92.650
(b)	99.017	91.557	93.583
(c)	98.683	89.929	92.300
(d) (Ours)	99.133	91.529	93.850

Table 7. Face recognition accuracy comparison of different parameters in Cross-Attention across LFW, CFP-FP, and AgeDB Datasets at 20k blurring intensity.

- (c) Similar to Experiment (d) but with the final Cross-Attention layer using the output of the first Cross-Attention (low-quality as Query) as the new Query.
- (d) (**Ours**) Two Cross-Attention layers are applied in succession—the first with high-quality as Query and low-quality as Key and Value, and the second reversing these roles. The final fusion feature is generated using the output of the first Cross Attention (high-quality as Query) as the new Query.

Table 7 shows the results of these experiments on the testing datasets. Our results indicate that model (d) has the best recognition scores on our test datasets. This outcome suggests that using the high-quality features as the base for the Query in the final fusion stage is more effective, possibly due to the richer and more discriminative information inherent in the high-quality features being leveraged to guide the fusion process. As shown in Fig. 4, the face information of the restored high-quality image is easier to be extracted by the face recognition model.

5. Conclusion

In this paper, we introduce a novel adapter framework to enhance face recognition in real-world scenarios with low-quality images. Our approach leverages a frozen pre-

trained model and a trainable adapter to bridge the gap between original and enhanced images. Specifically, the Fusion Structure integrates advanced nested Cross-Attention and Self-Attention mechanisms. The extensive experiments across multiple datasets show that our method significantly improves accuracy and reliability in face recognition than conventional techniques. This work sets a new standard in the field, offering a robust solution for varied applications and paving the way for future advancements in face recognition technologies. In the future, we would enhance our adapter framework to address more complex image quality issues, such as varying lighting and obstructions. We aim to adapt our approach for real-time applications, broadening its utility in fields like surveillance and mobile authentication.

References

- [1] Somaya Ali Al-Maadeed, Mehdi Bourif, Ahmed Bouridane, and Richard M. Jiang. Low-quality facial biometric verification via dictionary-based random pooling. *Pattern Recognit.*, 2016. 3
- [2] Mustamin Anggo and La Arapu. Face recognition using fisherface method. In *Journal of Physics: Conference Series*, 2018. 2
- [3] Simon Baker and Takeo Kanade. Hallucinating faces. *Proceedings Fourth IEEE International Conference on Automatic Face and Gesture Recognition*, 2000. 2
- [4] Ankan Bansal, Anirudh Nanduri, Carlos D Castillo, Rajeev Ranjan, and Rama Chellappa. Umdfaces: An annotated face dataset for training deep networks. In *IJCB*, 2017. 5
- [5] Peter N. Belhumeur, João Pedro Hespanha, and David J. Kriegman. Eigenfaces vs. fisherfaces: Recognition using class specific linear projection. In *ECCV*, 1996. 2
- [6] Xianye Ben, Ming Lang Jiang, Y. J. Wu, and Weixiao Meng. Gait feature coupling for low-resolution face recognition. *Electronics Letters*, 2012. 3
- [7] Soma Biswas, K. Bowyer, and Patrick J. Flynn. Multidimensional scaling for matching low-resolution face images. *TPAMI*, 2012. 3
- [8] Hong Chang, D. Y. Yeung, and Yimin Xiong. Super-resolution through neighbor embedding. *CVPR*, 2004. 2
- [9] Chaofeng Chen, Dihong Gong, Hao Wang, Zhifeng Li, and Kwan-Yee Kenneth Wong. Learning spatial attention for face super-resolution. *TIP*, 2020. 3
- [10] Yu Chen, Ying Tai, Xiaoming Liu, Chunhua Shen, and Jian Yang. Fsrnet: End-to-end learning face super-resolution with facial priors. *CVPR*, 2017. 3
- [11] Bowen Cheng, Alexander G. Schwing, and Alexander Kirillov. Per-pixel classification is not all you need for semantic segmentation. 2021. 3
- [12] Bowen Cheng, Ishan Misra, Alexander G. Schwing, Alexander Kirillov, and Rohit Girdhar. Masked-attention mask transformer for universal image segmentation. 2022. 3
- [13] Xiaojuan Cheng, Jiwen Lu, Bo Yuan, and Jie Zhou. Face segmentor-enhanced deep feature learning for face recognition. *IEEE Transactions on Biometrics, Behavior, and Identity Science*, 2019. 1, 2
- [14] Nicholas Chimitt and Stanley H. Chan. Simulating anisoplanatic turbulence by sampling intermodal and spatially correlated Zernike coefficients. *Optical Engineering*, 2020. 5, 2
- [15] Grigorios G. Chrysos and Stefanos Zafeiriou. Deep face deblurring. *CVPRW*, 2017. 3
- [16] Jiankang Deng, Yuxiang Zhou, and Stefanos Zafeiriou. Marginal loss for deep face recognition. *CVPRW*, 2017. 2
- [17] Jiankang Deng, Jia Guo, Niannan Xue, and Stefanos Zafeiriou. Arcface: Additive angular margin loss for deep face recognition. In *CVPR*, 2019. 1, 2, 3, 5, 6, 4
- [18] Qi Dou, Daniel Coelho de Castro, Konstantinos Kamnitsas, and Ben Glocker. Domain generalization via model-agnostic learning of semantic features. In *Neural Information Processing Systems*, 2019. 1
- [19] Yueqi Duan, Jiwen Lu, and Jie Zhou. Uniformface: Learning deep equidistributed representation for face recognition. *CVPR*, 2019. 2
- [20] Reuben A. Farrugia and Christine M. Guillemot. Face hallucination using linear models of coupled sparse support. *TIP*, 2015. 3
- [21] Jan Flusser, Sajad Farokhi, IV CyrilHöschl, Tomávs. Suk, Barbara Zitová, and Matteo Pedone. Recognition of images degraded by gaussian blur. *TIP*, 2016. 3
- [22] Guangwei Gao, Pu Huang, Quan Zhou, Zangyi Hu, and Dong Yue. Low-rank representation and locality-constrained regression for robust low-resolution face recognition. *Artificial Intelligence and Robotics*, 2018. 3
- [23] Xinbo Gao, N. Wang, Dacheng Tao, and Xuelong Li. Face sketch-photo synthesis and retrieval using sparse representation. *TCSVT*, 2012. 2
- [24] Jacob Gildenblat and contributors. Pytorch library for cam methods. <https://github.com/jacobgil/pytorch-grad-cam>, 2021. 7
- [25] Yuchao Gu, Xintao Wang, Liangbin Xie, Chao Dong, Gengyan Li, Ying Shan, and Ming-Ming Cheng. Vqfr: Blind face restoration with vector-quantized dictionary and parallel decoder. In *ECCV*, 2022. 1, 3
- [26] Kaiming He, X. Zhang, Shaoqing Ren, and Jian Sun. Delying deep into rectifiers: Surpassing human-level performance on imagenet classification. *2015 IEEE International Conference on Computer Vision (ICCV)*, pages 1026–1034, 2015. 1
- [27] Kaiming He, X. Zhang, Shaoqing Ren, and Jian Sun. Identity mappings in deep residual networks. In *European Conference on Computer Vision*, 2016. 1
- [28] Kaiming He, Xiangyu Zhang, Shaoqing Ren, and Jian Sun. Deep residual learning for image recognition. In *CVPR*, 2016. 3
- [29] Christian Herrmann. Extending a local matching face recognition approach to low-resolution video. *2013 10th IEEE International Conference on Advanced Video and Signal Based Surveillance*, 2013. 3
- [30] Yibo Hu, Xiang Wu, Bing Yu, Ran He, and Zhenan Sun. Pose-guided photorealistic face rotation. *CVPR*, 2018. 2

- [31] Gang Hua, Ming-Hsuan Yang, Erik G. Learned-Miller, Yi Ma, Matthew A. Turk, David J. Kriegman, and Thomas S. Huang. Introduction to the special section on real-world face recognition. *IEEE transactions on pattern analysis and machine intelligence*, 33 10:1921–4, 2011. 1
- [32] Gao Huang, Zhuang Liu, and Kilian Q. Weinberger. Densely connected convolutional networks. *2017 IEEE Conference on Computer Vision and Pattern Recognition (CVPR)*, pages 2261–2269, 2016. 1
- [33] Gary B Huang, Marwan Mattar, Tamara Berg, and Eric Learned-Miller. Labeled faces in the wild: A database for studying face recognition in unconstrained environments. In *Workshop on faces in 'Real-Life' Images: detection, alignment, and recognition*, 2008. 5, 2
- [34] Jian Huang, Junyi Chai, and Stella Cho. Deep learning in finance and banking: A literature review and classification. *Frontiers of Business Research in China*, 14:1–24, 2020. 1
- [35] Rui Huang, Shu Zhang, Tianyu Li, and Ran He. Beyond face rotation: Global and local perception gan for photorealistic and identity preserving frontal view synthesis. *ICCV*, 2017. 2
- [36] Y. Huang, Yuhan Wang, Ying Tai, Xiaoming Liu, Pengcheng Shen, Shaoxin Li, Jilin Li, and Feiyue Huang. Curricular-face: Adaptive curriculum learning loss for deep face recognition. *CVPR*, 2020. 2
- [37] Zeyi Huang, Haohan Wang, Eric P. Xing, and Dong Huang. Self-challenging improves cross-domain generalization. *ArXiv*, abs/2007.02454, 2020. 1
- [38] Zhizhong Huang, Junping Zhang, and Hongming Shan. When age-invariant face recognition meets face age synthesis: A multi-task learning framework. *CVPR*, 2021. 2
- [39] Zheng Hui, Xinbo Gao, Yunchu Yang, and Xiumei Wang. Lightweight image super-resolution with information multi-distillation network. *ACM MM*, 2019. 3
- [40] Junjun Jiang, Jiayi Ma, Chen Chen, Xinwei Jiang, and Zheng Wang. Noise robust face image super-resolution through smooth sparse representation. *IEEE Transactions on Cybernetics*, 2017. 3
- [41] Weiwei Jiang. Applications of deep learning in stock market prediction: recent progress. *Expert Syst. Appl.*, 184:115537, 2020. 1
- [42] Meiguang Jin, Michael Hirsch, and Paolo Favaro. Learning face deblurring fast and wide. *CVPRW*, 2018. 3
- [43] Y. Kim, Wonpyo Park, Myung-Cheol Roh, and Jongju Shin. Groupface: Learning latent groups and constructing group-based representations for face recognition. *CVPR*, 2020. 1, 2
- [44] Yann LeCun, Yoshua Bengio, and Geoffrey E. Hinton. Deep learning. *Nature*, 521:436–444, 2015. 1
- [45] Aijin Li, Gengyan Li, Lei Sun, and Xintao Wang. Face-former: Scale-aware blind face restoration with transformers. *ArXiv*, 2022. 1, 3
- [46] Bo Li, Hong Chang, S. Shan, and Xilin Chen. Low-resolution face recognition via coupled locality preserving mappings. *IEEE Signal Processing Letters*, 2010. 3
- [47] Pei Li, Loreto Prieto, Domingo Mery, and Patrick Flynn. Face recognition in low quality images: A survey. *arXiv preprint arXiv:1805.11519*, 2018. 3
- [48] Xiaoming Li, Wenyu Li, Dongwei Ren, Hongzhi Zhang, Meng Wang, and Wangmeng Zuo. Enhanced blind face restoration with multi-exemplar images and adaptive spatial feature fusion. *CVPR*, 2020. 1, 3
- [49] Yung-Hui Li, Marios Savvides, and B. V. K. Vijaya Kumar. Illumination tolerant face recognition using a novel face from sketch synthesis approach and advanced correlation filters. *ICASSP*, 2006. 2
- [50] Bingyu Liu, Weihong Deng, Yaoyao Zhong, Mei Wang, Jiani Hu, Xunqiang Tao, and Yaohai Huang. Fair loss: Margin-aware reinforcement learning for deep face recognition. *ICCV*, 2019. 2
- [51] Hao Liu, Xiangyu Zhu, Zhen Lei, and S. Li. Adaptive-face: Adaptive margin and sampling for face recognition. *2019 IEEE/CVF Conference on Computer Vision and Pattern Recognition (CVPR)*, pages 11939–11948, 2019. 1
- [52] Weiyang Liu, Yandong Wen, Zhiding Yu, and Meng Yang. Large-margin softmax loss for convolutional neural networks. In *ICML*, 2016. 2
- [53] Weiyang Liu, Yandong Wen, Zhiding Yu, Ming Li, Bhiksha Raj, and Le Song. Sphreface: Deep hypersphere embedding for face recognition. *CVPR*, 2017. 1, 2
- [54] Xiangyu Liu. Applicability of face recognition in real-world scenarios. In *2021 International Conference on Signal Processing and Machine Learning (CONF-SPML)*, pages 316–319, 2021. 1
- [55] Yu Liu, Junjie Yan, and Wanli Ouyang. Quality aware network for set to set recognition. *CVPR*, 2017. 2
- [56] Ali Moeini, Karim Faez, Hossein Moeini, and Armon Matthew Safai. Open-set face recognition across look-alike faces in real-world scenarios. *Image Vis. Comput.*, 57: 1–14, 2017. 1
- [57] Stylianos Moschoglou, Athanasios Papaioannou, Christos Sagonas, Jiankang Deng, Irene Kotsia, and Stefanos Zafeiriou. Agedb: the first manually collected, in-the-wild age database. In *CVPRW*, 2017. 5, 2
- [58] Lu Qi, Shu Liu, Jianping Shi, and Jiaya Jia. Sequential context encoding for duplicate removal. *NeurIPS*, 2018. 1
- [59] Lu Qi, Li Jiang, Shu Liu, Xiaoyong Shen, and Jiaya Jia. Amodal instance segmentation with kins dataset. In *CVPR*, 2019.
- [60] Lu Qi, Yi Wang, Yukang Chen, Ying-Cong Chen, Xiangyu Zhang, Jian Sun, and Jiaya Jia. Pointins: Point-based instance segmentation. *TPAMI*, 2021.
- [61] Lu Qi, Jason Kuen, Zhe Lin, Jiuxiang Gu, Fengyun Rao, Dian Li, Weidong Guo, Zhen Wen, Ming-Hsuan Yang, and Jiaya Jia. Ca-ssl: Class-agnostic semi-supervised learning for detection and segmentation. In *ECCV*, 2022.
- [62] Lu Qi, Jason Kuen, Yi Wang, Jiuxiang Gu, Hengshuang Zhao, Philip Torr, Zhe Lin, and Jiaya Jia. Open world entity segmentation. *TPAMI*, 2022.
- [63] Lu Qi, Jason Kuen, Weidong Guo, Jiuxiang Gu, Zhe Lin, Bo Du, Yu Xu, and Ming-Hsuan Yang. Aims: All-inclusive multi-level segmentation for anything. In *NeurIPS*, 2023.
- [64] Lu Qi, Jason Kuen, Tiancheng Shen, Jiuxiang Gu, Wenbo Li, Weidong Guo, Jiaya Jia, Zhe Lin, and Ming-Hsuan Yang. High quality entity segmentation. In *ICCV*, 2023. 1

- [65] Rajeev Ranjan, Carlos D Castillo, and Rama Chellappa. L2-constrained softmax loss for discriminative face verification. *arXiv preprint arXiv:1703.09507*, 2017. 2
- [66] Chuan-Xian Ren, Dao-Qing Dai, and Hong Yan. Coupled kernel embedding for low-resolution face image recognition. *TIP*, 2012. 3
- [67] Mohammad Saeed Ebrahimi Saadabadi, Sahar Rahimi Malakshan, Ali Zafari, Moktari Mostofa, and Nasser M. Nasrabadi. A quality aware sample-to-sample comparison for face recognition. In *WACV*, 2023. 6
- [68] Soumyadip Sengupta, Jun-Cheng Chen, Carlos Castillo, Vishal M Patel, Rama Chellappa, and David W Jacobs. Frontal to profile face verification in the wild. In *WACV*, 2016. 5, 2
- [69] Omer Berat Sezer, Mehmet Ugur Gudelek, and Ahmet Murat Ozbayoglu. Financial time series forecasting with deep learning : A systematic literature review: 2005-2019. *ArXiv*, abs/1911.13288, 2019. 1
- [70] Jin shan Pan, Deqing Sun, Hanspeter Pfister, and Ming-Hsuan Yang. Blind image deblurring using dark channel prior. *CVPR*, 2016. 2
- [71] Evan Shelhamer, Jonathan Long, and Trevor Darrell. Fully convolutional networks for semantic segmentation. *2015 IEEE Conference on Computer Vision and Pattern Recognition (CVPR)*, pages 3431–3440, 2014. 1
- [72] Ziyi Shen, Wei-Sheng Lai, Tingfa Xu, Jan Kautz, and Ming-Hsuan Yang. Deep semantic face deblurring. *CVPR*, 2018. 3
- [73] Karen Simonyan and Andrew Zisserman. Very deep convolutional networks for large-scale image recognition. *CoRR*, abs/1409.1556, 2014. 1
- [74] Nitish Srivastava, Geoffrey E. Hinton, Alex Krizhevsky, Ilya Sutskever, and Ruslan Salakhutdinov. Dropout: a simple way to prevent neural networks from overfitting. *J. Mach. Learn. Res.*, 15:1929–1958, 2014. 1
- [75] Yi Sun, Xiaogang Wang, and Xiaoou Tang. Hybrid deep learning for face verification. *2013 IEEE International Conference on Computer Vision*, pages 1489–1496, 2013. 1
- [76] Yi Sun, Yuheng Chen, Xiaogang Wang, and Xiaoou Tang. Deep learning face representation by joint identification-verification. *ArXiv*, abs/1406.4773, 2014. 1
- [77] Yifan Sun, Changmao Cheng, Yuhang Zhang, Chi Zhang, Liang Zheng, Zhongdao Wang, and Yichen Wei. Circle loss: A unified perspective of pair similarity optimization. *CVPR*, 2020. 2
- [78] Nima Tajbakhsh, Jae Y. Shin, Suryakanth R. Gurudu, R. Todd Hurst, Christopher B. Kendall, Michael B. Gotway, and Jianming Liang. Convolutional neural networks for medical image analysis: Full training or fine tuning? *IEEE Transactions on Medical Imaging*, 35(5):1299–1312, 2016. 1
- [79] Luan Tran, Xi Yin, and Xiaoming Liu. Disentangled representation learning gan for pose-invariant face recognition. *CVPR*, 2017. 2
- [80] Feng Wang, Jian Cheng, Weiyang Liu, and Haijun Liu. Additive margin softmax for face verification. *IEEE Signal Processing Letters*, 2018. 2
- [81] H. Wang, Yitong Wang, Zheng Zhou, Xing Ji, Zhifeng Li, Dihong Gong, Jin Zhou, and Wei Liu. Cosface: Large margin cosine loss for deep face recognition. *CVPR*, 2018. 1, 2, 6
- [82] N. Wang, Xinbo Gao, Dacheng Tao, and Xuelong Li. Face sketch-photo synthesis under multi-dictionary sparse representation framework. *2011 Sixth International Conference on Image and Graphics*, 2011. 2
- [83] Qiangchang Wang, Tianyi Wu, He Zheng, and Guodong Guo. Hierarchical pyramid diverse attention networks for face recognition. *CVPR*, 2020. 1, 2
- [84] Xiaoying Wang, Haifeng Hu, and Jianquan Gu. Pose robust low-resolution face recognition via coupled kernel-based enhanced discriminant analysis. *IEEE/CAA Journal of Automatica Sinica*, 2016. 3
- [85] Xintao Wang, Yu Li, Honglun Zhang, and Ying Shan. Towards real-world blind face restoration with generative facial prior. *CVPR*, 2021. 3
- [86] Zhaowen Wang, Ding Liu, Jianchao Yang, Wei Han, and Thomas S. Huang. Deep networks for image super-resolution with sparse prior. *ICCV*, 2015. 3
- [87] Zhenyu Wang, Wankou Yang, and Xianye Ben. Low-resolution degradation face recognition over long distance based on cca. *Neural Computing and Applications*, 2015. 3
- [88] Zhouxia Wang, Jiawei Zhang, Runjian Chen, Wenping Wang, and Ping Luo. Restoreformer: High-quality blind face restoration from undegraded key-value pairs. *CVPR*, 2022. 1
- [89] Zhouxia Wang, Jiawei Zhang, Runjian Chen, Wenping Wang, and Ping Luo. Restoreformer: High-quality blind face restoration from undegraded key-value pairs. 2022. 3, 6, 2
- [90] Yanyang Yan, Wenqi Ren, Yuanfang Guo, Rui Wang, and Xiaochun Cao. Image deblurring via extreme channels prior. *CVPR*, 2017. 2
- [91] Jiaolong Yang, Peiran Ren, Dongqing Zhang, Dong Chen, Fang Wen, Hongdong Li, and Gang Hua. Neural aggregation network for video face recognition. *CVPR*, 2016. 1, 2
- [92] Tao Yang, Peiran Ren, Xuansong Xie, and Lei Zhang. Gan prior embedded network for blind face restoration in the wild. *CVPR*, 2021. 1, 3
- [93] Matthew D. Zeiler and Rob Fergus. Visualizing and understanding convolutional networks. *ArXiv*, abs/1311.2901, 2013. 1
- [94] Lu Zhang, Lu Qi, Xu Yang, Hong Qiao, Ming-Hsuan Yang, and Zhiyong Liu. Automatically discovering novel visual categories with adaptive prototype learning. *TPAMI*, 2023. 1
- [95] Xiao Zhang, Rui Zhao, Yu Qiao, Xiaogang Wang, and Hongsheng Li. Adacos: Adaptively scaling cosine logits for effectively learning deep face representations. *CVPR*, 2019. 2
- [96] Shangchen Zhou, Kelvin C.K. Chan, Chongyi Li, and Chen Change Loy. Towards robust blind face restoration with codebook lookup transformer. In *NeurIPS*, 2022. 3, 5, 2
- [97] Zongwei Zhou, Jae Shin, Lei Zhang, Suryakanth Gurudu, Michael Gotway, and Jianming Liang. Fine-tuning convolutional neural networks for biomedical image analysis: Ac-

tively and incrementally. In *Proceedings of the IEEE Conference on Computer Vision and Pattern Recognition (CVPR)*, 2017. [1](#)

- [98] Feida Zhu, Junwei Zhu, Wenqing Chu, Xinyi Zhang, Xiaozhong Ji, Chengjie Wang, and Ying Tai. Blind face restoration via integrating face shape and generative priors. *CVPR*, 2022. [3](#)

Effective Adapter for Face Recognition in the Wild

Supplementary Material

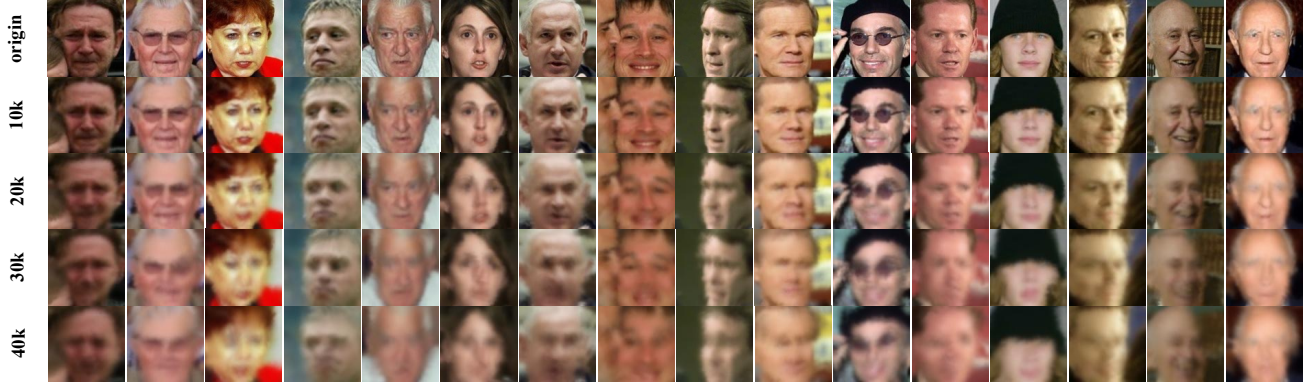


Figure 7. Comparative analysis of image degradation under varying turbulence intensities. This figure presents a series of images processed using the TurbulenceSim tool, showcasing the effects of atmospheric turbulence at distinct parameters: 10k, 20k, 30k, and 40k meters, as well as the origin images without degradation. Each row or set of images corresponds to one of these parameters, illustrating the progressive impact on image quality as the turbulence intensity increases.

6. Tools of Image Processing

Image Degradation. Image degradation refers to the process of quality reduction in an image, often encountered in real-world scenarios. Common causes of degradation include noise, blur, poor lighting, and compression artifacts. In the context of face recognition in the wild, these factors significantly challenge the recognition accuracy. Understanding the types and sources of degradation is crucial in developing robust face recognition systems. This includes, but is not limited to, Gaussian blur, which simulates out-of-focus images; salt-and-pepper noise, representing random pixel intensity disruptions; and motion blur, a result of rapid movement during image capture. Analyzing these degradation types helps in simulating real-world conditions for model training and evaluation.

In our study, we particularly focus on image degradation caused by atmospheric turbulence, which is a significant challenge in outdoor face recognition scenarios. Our methodology for simulating image degradation involves a sophisticated model of atmospheric turbulence, particularly focusing on the impact of this turbulence on long-distance face recognition. To simulate this type of degradation, we employ TurbulenceSim [14]. TurbulenceSim realistically models the distortion effects caused by atmospheric turbulence, such as blurring and warping, which are common in images captured in long-range surveillance or outdoor environments. It replicates the atmospheric conditions by modeling the distortion effects like blurring and warping, which are typical in long-range surveillance or outdoor en-

vironments. The simulation involves multiple steps, as it is shown in Table 8.

Our image degradation model includes four distinct parameters: $meters = 10k, 20k, 30k, 40k$. These parameters represent the turbulence intensity in the algorithm, providing a range of scenarios from mild to severe atmospheric conditions. In Fig. 7, we compare images processed under these different distinct parameters. This comparison demonstrates the varying effects of turbulence intensity on image quality. We use LFW [33], CFP-FP [68], and AgeDB [57] as our evaluation dataset.

Image Restoration. In the process of restoring degraded images, our study employs two methodologies: Codeformer [96] and Restoreformer [89]. These tools enhance the quality of images affected by atmospheric turbulence, thereby generating the HQ images as one of the inputs of our method. In particular, there is a fidelity weight parameter w in Codeformer, which we vary across three different settings: $w = 0.0, 0.5$, and 1.0 . The fidelity weight w lies in the range $[0, 1]$, where a smaller w value generally produces a higher-quality result, and a larger w value yields a result with higher fidelity to the original degraded image. This flexibility allows us to balance between enhancing image quality and maintaining the authenticity of the original features.

In our experimental setup, we compare the performance of images restored using Codeformer with the three different fidelity weight parameters and Restoreformer. This comparison is important to understand how different restoration methods and parameter settings affect the over-

Serial	Name	Intro
1	Parameter Initialization	Involves setting up essential simulation parameters like image size, aperture diameter, propagation length, Fried parameter, and wavelength.
2	Power Spectral Density (PSD) Generation	Creates the PSD for tilt values, essential for simulating pixel shifts due to turbulence.
3	Image Tilt and Blur	Applies PSD to the input image to produce a tilted version, followed by the generation of a blurred image to mimic turbulence effects.
4	Zernike Coefficients	Generates Zernike coefficients for modeling wavefront distortions caused by atmospheric turbulence.
5	Processing Pipeline	Processes the images through the turbulence model, first tilting and then blurring them to create a realistic dataset for face recognition challenges.

Table 8. Summary of TurbulenceSim method steps



Figure 8. Comparative evaluation of image restoration methods. This figure illustrates the effectiveness of different image restoration approaches on degraded facial images. CF refers to Codeformer, and RF refers to Restoreformer. For Codeformer, three distinct fidelity weight parameters ($w = 0.0, 0.5, 1.0$) are evaluated, demonstrating how varying levels of fidelity weights impact the restoration quality.

Param	d_model	nhead	dropout	bias
Value	512	8	0.0	True

Table 9. This table enumerates the specific parameters used in the nn.MultiheadAttention layer within both Cross-Attention and Self-Attention components of our Fusion Structure. The parameters include d_model (dimension of the model), nhead (number of attention heads), dropout rate, and whether bias is included.

all quality and fidelity of the restored images. It also provides insights into the optimal restoration strategy for enhancing the performance of face recognition systems in wild scenarios. Fig. 8 presents a comprehensive comparison of images restored using these methods. It showcases the distinct outcomes of each setting of Codeformer and the results achieved using Restoreformer.

7. Fusion Structure

The Fusion Structure in our study plays an important role in integrating and processing features from both restored and original degraded images. The **codebase** for this model is primarily derived from [11, 12].

Cross-Attention. As it is shown in Fig. 9 (a), Cross-Attention is designed to integrate features from both the restored and original image streams. This integration is essential for the model to effectively understand and interpret faces in varying conditions. By aligning and correlating features from the dual inputs, Cross-Attention ensures that the combined feature set is and comprehensive, enhancing the face recognition system’s ability to adapt to diverse image qualities.

Self-Attention. As it is shown in Fig. 9 (b), Self-Attention is utilized to process the input features. By modeling and associating these features, the mechanism captures the global contextual information of the image. This approach enables the model to consider the entire image’s contextual infor-

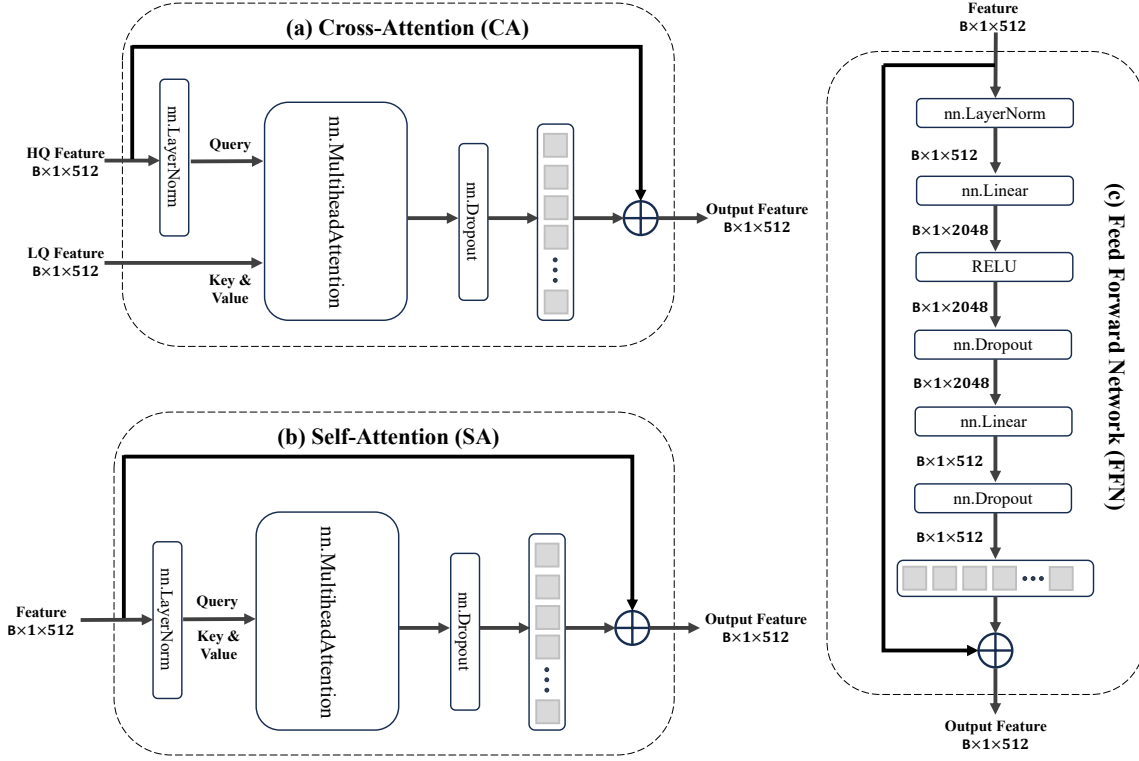


Figure 9. **Detailed Illustration of Fusion Structure Components.** This figure provides a visual representation of the three key parts of our Fusion Structure: (a) Cross-Attention, (b) Self-Attention, and (c) Feed Forward Network. Each diagram in the figure meticulously details the layers involved, along with the inputs and outputs of these respective components. In both (a) and (b), we use the same parameters to initialize the method `nn.MultiheadAttention`, as it is shown in Table 9. The Cross-Attention diagram (a) showcases how features from different image streams are integrated, while the Self-Attention diagram (b) illustrates the processing of features within a single image stream. Lastly, the Feed Forward Network diagram (c) depicts the sequential layers responsible for refining and preparing the final feature output.

mation. Consequently, richer features essential for effective face recognition are extracted, thereby improving the accuracy of the system.

Feed Forward Network. As it is shown in Fig. 9 (c), Feed Forward Network (FFN) acts as the final processing stage in the network, refining the features post-attention processing. It consists of multiple dense layers that further enhance the feature set, ensuring that the final output is well-suited for the face recognition task.

8. Results of Visualization

In this section, we present the results of our visualization experiments, designed to compare the performance of the traditional Arcface [17] method with our method in face recognition, especially when dealing with low-quality images. These visualization experiments are crucial for demonstrating the practical effectiveness of our method in real-world scenarios where image quality often varies.

For the probe images in our experiments, we employ the

parameter `TurbulenceSim` $m = 20k$ to blur the images. Subsequently, we use Codeformer with a fidelity weight $w = 0.5$ to restore the images.

Our comparison is based on the use of cosine similarity as a metric to determine the degree of similarity between the gallery feature and the probe feature. The formula for calculating the cosine similarity of two vectors s_1 and s_2 is defined as:

$$\text{Cosine Similarity}(s_1, s_2) = \frac{s_1 \cdot s_2}{\|s_1\| \|s_2\|} \quad (6)$$

Where \cdot denotes the dot product of the two vectors, and $\|s_1\|$ and $\|s_2\|$ are the magnitudes of vectors s_1 and s_2 , respectively.

Image Pair Score Comparison. In this experiment, we delve into a detailed comparative analysis between the Arcface method and our proposed method using a 1 : 1 image pair approach. This comparison is visually represented in Fig. 10. In this experimental setup, pairs of images are used to evaluate the effectiveness of both methods in recognizing

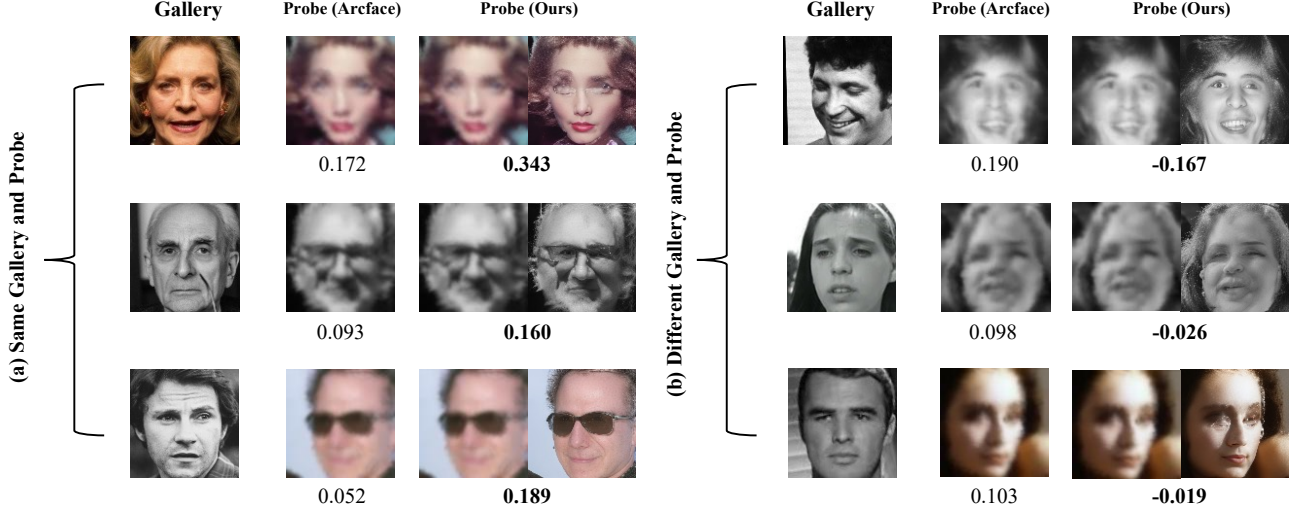


Figure 10. Comparative analysis of face recognition methods on image pair. (a) illustrates the comparison results using different methods on an image pair of the same person, while (b) presents the results for an image pair of different people. Each image pair is accompanied by a cosine similarity score, ranging from -1 to 1 , where a higher score indicates greater similarity between the images, and vice versa.

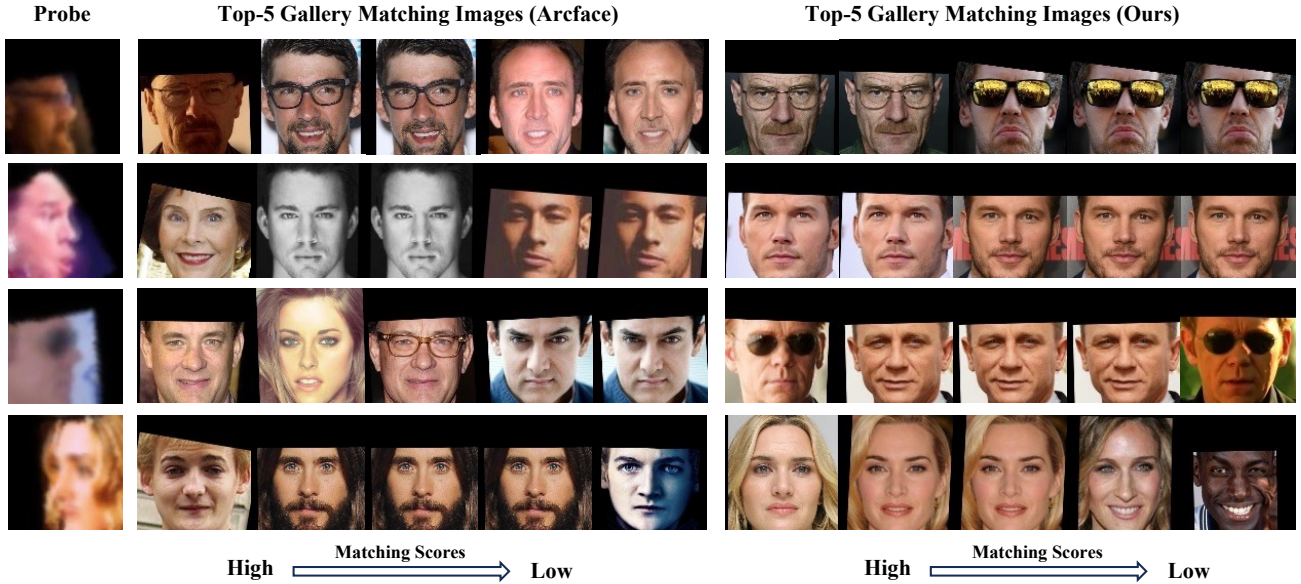


Figure 11. Comparative analysis of face recognition methods on $1 : N$ matching. This figure displays the Top 5 matching results for blurred face probes using both Arcface and our method. Each line contains an input probe and the Top 5 matches of the gallery using each of the two methods.

and verifying the same individual. Each pair consists of two images, one serving as a gallery and the other as a probe.

Our experimental results demonstrate that the features extracted by our method are more representative of the key characteristics of the face. This enhanced representation leads to a more accurate determination of whether the two images in a pair represent the same person.

Top-K People. In this experiment, we explore the comparison between the Arcface method and our proposed approach using a $1 : N$ methodology. This approach is key to understanding the performance of face recognition methods in scenarios where a single input (probe) face is compared against a larger database (gallery) of faces.

In our experimental setup, we introduce blurred input

face probes. These probes are then matched against a pre-established gallery of original, high-quality face images. Fig. 11 presents the results of these experiments, showing the Top 5 matches for each probe image as identified by both methods. The experimental data show that our method consistently ranks the correct individual higher in the list of potential matches compared to Arcface, thereby underlining its efficacy in practical, real-world face recognition applications where image quality can vary significantly.